

Article

Effect of the Water Hardness Level on Chalcopyrite Flotation Inhibition by the Disodium Carboxymethyl Trithiocarbonate

Yonghai Wang^{1,2}, Weiming Wu³, Yanhai Shao^{3,*}, Wenqing Qin¹  and Luzheng Chen³ ¹ School of Minerals Processing & Bioengineering, Central South University, Changsha 410083, China² Xi'an Northwest Nonferrous Geological Research Institute Co., Ltd., Xi'an 710054, China³ Faculty of Land Resource Engineering, Kunming University of Science and Technology, Kunming 650093, China

* Correspondence: shaoyanhai@kust.edu.cn; Tel.: +86-152-0871-6867

Abstract: Disodium carboxymethyl trithiocarbonate (DCMT) is considered to have the potential to replace sulfide and cyanide as a new chalcopyrite inhibitor. However, the effect of its application in the industrial field is often not ideal, mainly because the flotation involves solid, liquid and gas three-phase flotation systems, leading to many influencing factors, especially the chemical changes in pulp caused by the liquid phase. In order to promote the industrial application DCMT, we studied the effect of water quality in the flotation liquid phase on the inhibition of DCMT on chalcopyrite. Water quality generally involves the physical, chemical and biological characteristics of water bodies. The water for beneficiation belongs to industrial water, and the main indicator of its water quality is the water hardness level. Flotation and contact angle studies showed that higher water hardness levels suppressed chalcopyrite inhibition by DCMT. Infrared and Raman spectra revealed that the free CO_3^{2-} and Ca^{2+} in water coordinated with the residual organic chains on the surface of the pretreated chalcopyrite and was subsequently adsorbed onto the chalcopyrite surface. Moreover, the addition of DCMT dislodged the captured CO_3^{2-} and Ca^{2+} . X-ray photoelectron spectroscopy indicated that DCMT could adsorb on the chalcopyrite surface and compete with the Ca^{2+} . When Ca^{2+} was trapped on the chalcopyrite surface, there were fewer adsorption sites available to the DCMT, resulting in a lower inhibition capacity. Simultaneously, the presence of DCMT promoted the release of Ca^{2+} from the chalcopyrite surface. Therefore, the influence of water quality must be considered when designing a flotation reagent system, and the water hardness level should be reduced to optimize the flotation process.

Keywords: water hardness level; water quality; flotation; disodium carboxymethyl trithiocarbonate; chalcopyrite; pretreatment



Citation: Wang, Y.; Wu, W.; Shao, Y.; Qin, W.; Chen, L. Effect of the Water Hardness Level on Chalcopyrite Flotation Inhibition by the Disodium Carboxymethyl Trithiocarbonate. *Separations* **2023**, *10*, 375. <https://doi.org/10.3390/separations10070375>

Academic Editor: Sascha Nowak

Received: 30 May 2023

Revised: 21 June 2023

Accepted: 22 June 2023

Published: 26 June 2023



Copyright: © 2023 by the authors. Licensee MDPI, Basel, Switzerland. This article is an open access article distributed under the terms and conditions of the Creative Commons Attribution (CC BY) license (<https://creativecommons.org/licenses/by/4.0/>).

1. Introduction

Water is a commonly used medium in many mineral processing methods and is especially important in the flotation process, in which it serves as the liquid phase in a solid–liquid–gas flotation system [1]. The quality of water is determined by its physical (including turbidity, odor, and conductivity), chemical (organic and inorganic content), and biological (microorganisms) characteristics and composition [2–4]. In the flotation process, water quality is an important influencing factor [5]. The water used in mineral processing is classified as industrial water in which the primary water quality concern is the water hardness level. The water hardness level is determined by the concentrations of Ca^{2+} and Mg^{2+} in water [6] and can be classified into five grades based on the calcium carbonate content (Water Quality Association, WQA 2018), as summarized in Table 1.

Table 1. Relationship between calcium carbonate dosage and water hardness level (Water Quality Association, WQA 2018).

Water Hardness Level	Soft	Slightly Hard	Moderately Hard	Hard	Very Hard
CaCO ₃ (mg/L)	<17.0	17.0–59	60–119	120–180	>180

Chalcopyrite (CuFeS₂) is a common sulfide ore that is often associated with other sulfide ores such as molybdenite, galena, and sphalerite and clay gangue minerals [7–10]. When processing these ores, several minerals are typically mixed in the initial flotation step, followed by separation of the mixed flotation concentrate. While processing the copper–molybdenum ore, chalcopyrite and molybdenite are generally floated together to obtain a copper–molybdenum mixed concentrate. Copper and molybdenum are then separated from the copper–molybdenum mixed concentrate [11]. The common processing method for copper–lead–zinc ore involves preferentially floating copper and lead and then separating them [12]. The flotation separation stage in the processing of chalcopyrite and other sulfide ores cannot be avoided; therefore, the selection of a chalcopyrite inhibitor is particularly important. Many studies have examined chalcopyrite inhibitors, primarily focusing on organic substances, such as pseudo-glycolylthiourea [13], 4-amino-5-mercapto-1,2,4-triazole [14], and disodium carboxymethyl trithiocarbonate (DCMT) [15]. DCMT has attracted significant attention because of its two polar functional groups (-COO⁻ and -C=S) [16,17]. DCMT is a small molecular organic compound with a molecular weight of 212. DCMT has attracted significant attention because of its two polar functional groups (-COO⁻ and -C=S). DCMT can be used as a water agent. Existing studies have demonstrated DCMT's potential to replace sulfide and cyanide in the process of copper molybdenum separation, but there are still some aspects that require further research: (1) The origin of the copper molybdenum ore is different, which gives rise to different mineral characteristics. For example, the types and occurrence states of gangue minerals in the ore vary, and the reagent system and process adopted by the concentrator also vary, resulting in different residual reagents in the pulp, pulp potential, ion concentration in the pulp and dissolved oxygen during copper molybdenum separation, thus affecting the use of DCMT. (2) Simon Timbillah [13,16,18] showed that DCMT can mask the hydrophobic end of ethyl xanthate through the hydrophilic end, so as to make the surface of chalcopyrite hydrophilic, which is significant when selecting xanthate collectors when using DCMT. However, the copper inhibition mechanism of DCMT is not optimal, which limits the industrial application of DCMT. (3) At present, DCMT is mainly used in the form of a water solvent, and the purity of main components is not high; when the copper content in the mineral is particularly high, its inhibition effect is limited, which is one of the reasons why Yin et al. found it difficult to increase the molybdenum grade to more than 45%. (4) The separation of copper and molybdenum using DCMT as the inhibitor is conducted in an aqueous medium, but the effect of water quality on the flotation separation process has not been reported. Therefore, research on DCMT still requires further improvements [18–21]. However, DCMT yielded unsatisfactory results in industrial applications because the DCMT mechanism is not well-understood owing to the lack of recent DCMT research. This study focused on the DCMT mechanism and compared the flotation index of DCMT to those of traditional chalcopyrite inhibitors. DCMT can cover hydrophobic ethyl xanthate and remain adsorbed on the chalcopyrite surface, resulting in a hydrophilic chalcopyrite surface. DCMT is advantageous for inhibiting the chalcopyrite effect and is more cost-effective than traditional inhibitors. The effect of DCMT on the entire flotation, including the residual reagent on the surface of chalcopyrite after mixed flotation, was beyond the scope of this study. Thus, this effect on the entire flotation system requires additional research before the system can be applied in industrial processes.

This study focused on the inhibition behavior of DCMT on pretreated chalcopyrite under different water hardness levels to better guide the use of DCMT in the flotation process. In this study, the chalcopyrite treatment simulated the current industrial mixed flotation of chalcopyrite. Building on previous studies, the influence of water on the inhibition of chalcopyrite by DCMT was studied. Single-mineral flotation, powder contact angle testing, Fourier transform infrared spectroscopy (FT-IR), Raman spectroscopy, X-ray photoelectron spectroscopy (XPS), and contact angle studies were used to study the DCMT inhibition effect on chalcopyrite.

2. Materials and Methods

2.1. Materials and Reagents

Chalcopyrite was purchased from Guangdong Province. Table 2 and Figure 1 illustrate the multi-element chemical analysis and X-ray diffractometry results, respectively. The purity of the chalcopyrite (CuFeS_2) sample was calculated as 98 wt% based on the assumption that all the copper within CuFeS_2 met the pure mineral test requirements. After the chalcopyrite was crushed with an RK-PEW60 \times 100 pollution-free jaw crusher, particles with a size range of 0.6–3.5 mm were sieved and frozen.

Table 2. Chemical multi-element analysis of Chalcopyrite.

Element	Cu	Fe	S	Al_2O_3	CaO	Bi
Content/%	34.36	30.60	35.37	<0.5	0.34	0.0069

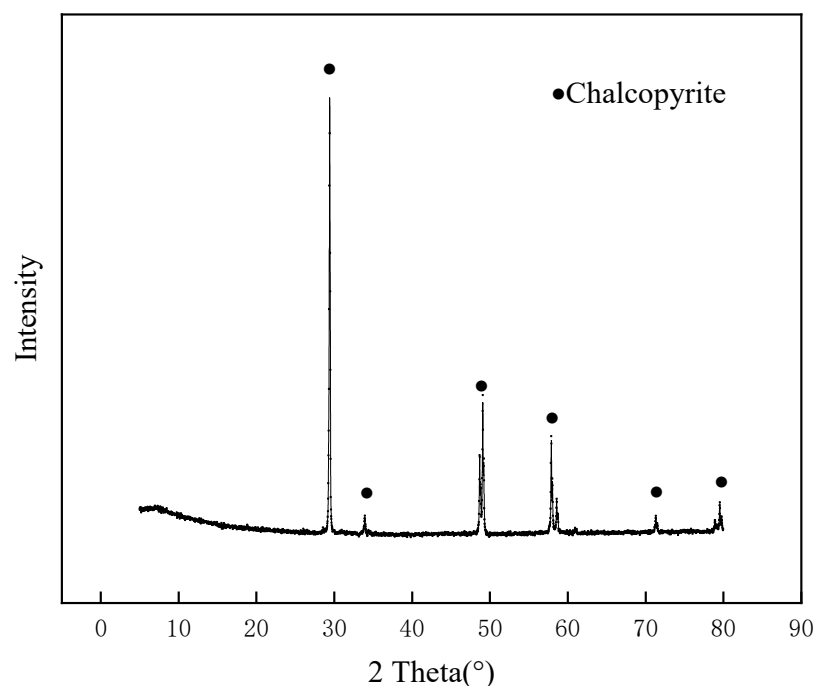


Figure 1. Chalcopyrite XRD.

DCMT was synthesized using previously reported methods [16,20]. The attenuated total reflectance-Fourier transform infrared (ATR-FTIR) spectrum of DCMT (Figure 2), shows the antisymmetric expansion (1634 cm^{-1}) and weak symmetric expansion (1380 cm^{-1}), respectively, of COO^- , and the weak $\text{C}=\text{S}$ expansion vibration ($1200\text{--}975\text{ cm}^{-1}$).

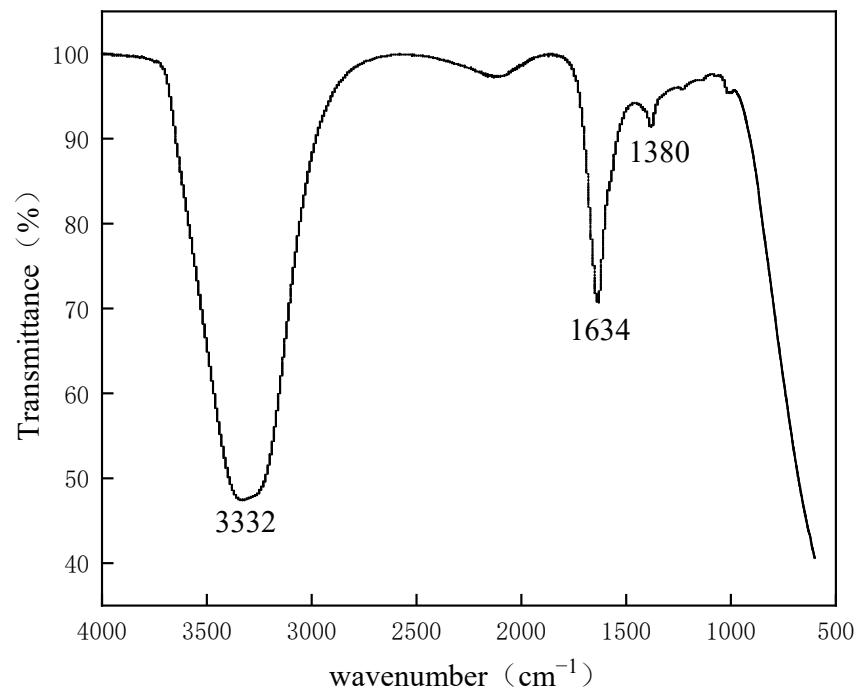


Figure 2. ATR-FTIR spectra of DCMT.

2.2. Methods

2.2.1. Grinding and Flotation

An XMQ-F150×50 conical ball mill was used to grind the samples. A total of 100 g aliquots of chalcopyrite were ground at a grinding concentration of 50%. After washing with a fixed volume of deionized water to obtain the grinding products, a screening test was conducted to determine the relationship between grinding fineness and time. The data-processing results are shown in Figure 3. The abscissa represents the grinding time t , and the ordinate R represents the weight percentage of -0.074 mm particle size fraction in grinding products. As seen in Figure 3, when grinding was conducted for 7 min, the percentage of grinding products with a particle size of -0.074 mm was 80%.

The process for the preparation of chalcopyrite used within this study is described as follows: (1) Chalcopyrite was crushed to a size of 0.6–3.5 mm using an RK-PEW60×100 pollution-free jaw crusher; (2) An XMQ-F150×50 conical ball mill was subsequently used to grind the particles to a size of -0.0074 mm; (3) After flotation with starch (depressant), ethyl xanthate (collector), and terpineol oil (frother), the sample was dehydrated and frozen. A multi-purpose vacuum filter (XTLZΦ260Φ200, Wuhan, China) is used for filtration and a vacuum-drying oven (DFZ-6020, Shanghai, China) is used for drying; then, the chalcopyrite sample is stored in a freezer at -15 °C to minimize further oxidation.

An RK/FD III 1.5 L single-cell flotation machine was used for flotation. One hundred grams of treated chalcopyrite were inserted into the flotation cell. After adding water with different hardness levels, the speed was set to 1900 r/min, the mixture was slurried for 2 min, and then DCMT (depressant) and kerosene (collector) were added successively for 5 min and 3 min, respectively. Terpineol oil (frother) was then added, and the machine was operated for 30 s before the charging valve was opened to inject gas into the slurry at a speed of 0.1 m³/min. Blistering occurred 1 min after the terpineol oil was added. The foam was scraped every 10 s, and four concentrates were collected after accumulation times of 1, 3, 6, and 10 min. The total weight of the four concentrates and the tailings was taken as the four concentrates are filtered, dried and weighed separately. The tailings were then filtered and weighed. The sum of the weight of the four concentrates and the tailings was taken as the total weight. Calculate the recovery rate for each time period separately. Use the cumulative recovery rate when graphing. Because this experiment

focused on the water hardness levels, the adjustment of the pulp pH was not included in this study. The initial pulp pH value was 5~6. Owing to the high purity of the chalcopyrite sample, the chalcopyrite recovery in the chalcopyrite flotation was calculated using the mass percentage. Each flotation test was repeated twice, and the average value was taken.

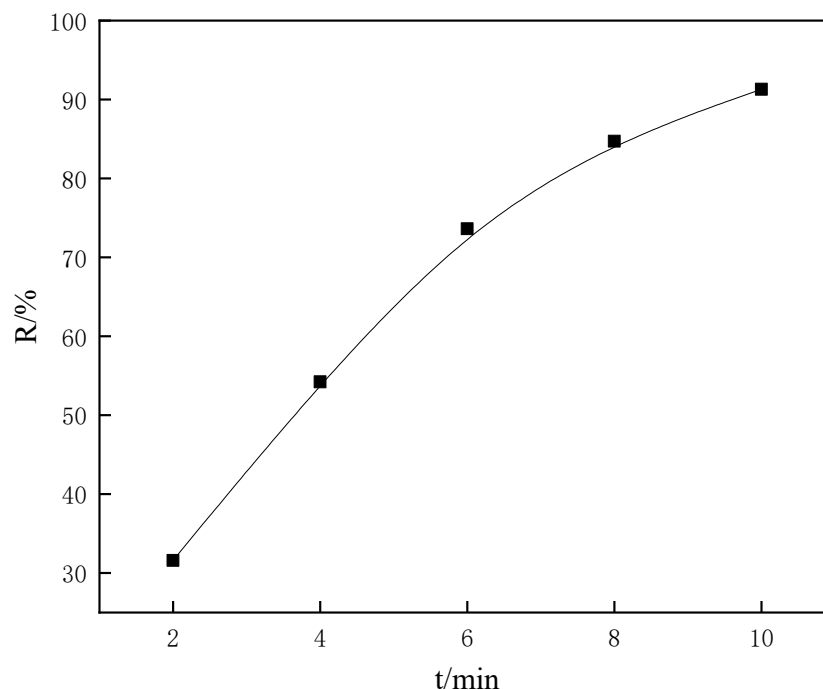


Figure 3. Effect of grinding time on grinding fineness.

2.2.2. Contact Angle

The contact angle can be a direct indicator of mineral wettability. To study the influence of the water hardness level on the floatability of chalcopyrite, samples taken before and after DCMT/kerosene flotation were used for the powder contact angle measurements. Twenty grams of the ore sample were weighed and placed in a 200 mL beaker and 100 mL of deionized water was added. After adding calcium carbonate, the sample was stirred for 3 min, filtered, and dried. The powder contact angle was tested using a fully automatic surface tension meter (Kruss GmbH, Hamburg, Germany). Each set of experiments was divided into two parts: (1) the capillary equivalent of chalcopyrite in an alcohol system was measured; and (2) the contact angle of chalcopyrite powder in a water system was measured under fixed capillary equivalent conditions. Each set was repeated three times and the average value was taken.

2.2.3. FT-IR Spectroscopy

For the FT-IR measurements, 2 g samples of the chalcopyrite, after undergoing the same flotation treatment, were placed into three beakers. Subsequently, 150 mL of deionized water was added to the three beakers, and two portions of calcium carbonate of the same quality were added to two of the beakers. The three beakers were then magnetically stirred for 30 min, filtered, washed with deionized water three times, and dried. A total of 10 mL of DCMT was added to a centrifuge tube and a dry calcium-carbonate-treated sample was placed into the centrifuge tube. This was then shaken for 10 min, filtered, washed three times with deionized water, and dried. The samples were then taken to a dry environment, placed into a mortar, ground together with an appropriate amount of dry KBr powder, and then placed into a tablet press to press transparent sheets. A Thermo Scientific Nicolet iS20 FT-IR spectrometer was used for the analysis. During the analysis, the background was collected prior to collecting the infrared spectrum of the sample. The resolution was 4 cm^{-1} and 32 scans were conducted in the wavenumber range of $400\text{--}4000\text{ cm}^{-1}$.

2.2.4. Raman Spectroscopy

The sample preparation was the same as that used for the FT-IR samples. Two-gram samples of the chalcopyrite, after undergoing the same flotation treatment, were placed into three beakers. Subsequently, 150 mL of deionized water was added to the three beakers, and two portions of calcium carbonate of the same quality was added to two of the beakers. The three beakers were then magnetically stirred for 30 min, filtered, washed with deionized water three times, and dried. A total of 10 mL of DCMT was added to a centrifuge tube and a dry calcium–carbonate-treated sample was placed into the centrifuge tube. This was then shaken for 10 min, filtered, washed three times with deionized water, and dried. A Horiba Scientific LabRAM HR Evolution (Tokyo, Japan) spectrometer was used to collect the Raman spectra. The laser wavelength was 325 nm, the wavenumber range was 50–4000 cm^{-1} , and three points were tested. Origin software was used for the fitting analysis.

3. Results and Discussion

3.1. Flotation Tests

Different hardness conditions were simulated based on the standard classification for water hardness. Simulated waters containing 0 mg/L CaCO_3 (soft water), 30 mg/L CaCO_3 (slightly hard water), 90 mg/L CaCO_3 (moderately hard water), 150 mg/L CaCO_3 (hard water), and 210 mg/L CaCO_3 (very hard water) were prepared according to the modified literature methods [22]. The DCMT dosage was fixed at 4000 g/t, and the test results are shown in Figure 4. The flotation test results indicated that the flotation recovery of chalcopyrite increases as the water hardness level increases. In a certain DCMT inhibitor system, the cumulative recovery of chalcopyrite under soft water is about 75%, the recovery of chalcopyrite under slightly water is about 79%, the recovery of chalcopyrite under moderately hard water is about 81%, the recovery of chalcopyrite under hard water is about 82%, and the recovery of chalcopyrite under very hard water, compared with the recovery of chalcopyrite under soft water, rises by nearly 10%. Furthermore, the flotation test results indicated a high recovery; therefore, it was necessary to verify whether the high recovery was due to the harder water by conducting a DCMT dosage change test. The results are shown in Figure 5. In the deionized water system, when the amount of DCMT was less than 4000 g/t (1000 g/t) and the recovery rate was about 90%, but when the amount of DCMT was more than 4000 g/t (8000 g/t), the recovery rate was about 60%. As the dosage increased, the inhibition effect of DCMT was enhanced, which confirms that the DCMT exhibited an inhibitory effect.

Calcium carbonate is thought to promote the recovery of chalcopyrite for the following reasons: (1) The addition of calcium carbonate changes the pH and Eh of the pulp, affecting the flotation recovery of chalcopyrite [23–25]; (2) The residual starch on the surface of the chalcopyrite reacts with the added calcium ions and adsorbs on the surface of the chalcopyrite, which impacts the inhibition of chalcopyrite by DCMT. Studies have shown that metal ions in the solution can be adsorbed on the mineral surface through ion exchange or chelation and affect the interaction between the flotation agents and minerals, particularly silicates [26–29]. Although there are few studies on the adsorption of calcium ions on the surface of chalcopyrite at present, the chalcopyrite in this study is in a particulate state, and reagents residues may remain after the initial washing process. Additionally, studies have shown that starch participates in acid–base reactions with metal hydroxyl compounds [30,31].

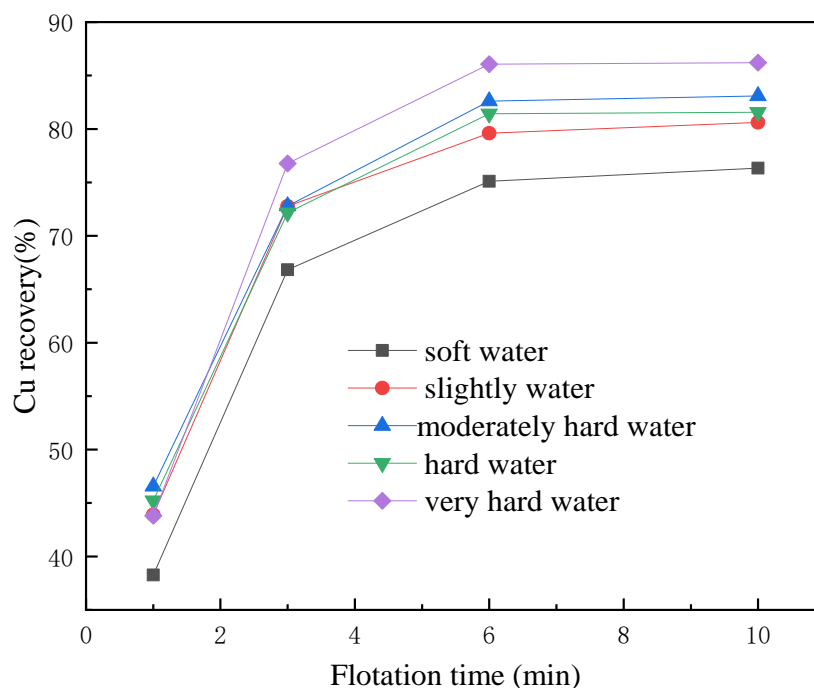


Figure 4. Chalcopyrite recovery as a function of flotation time in different water hardness levels.

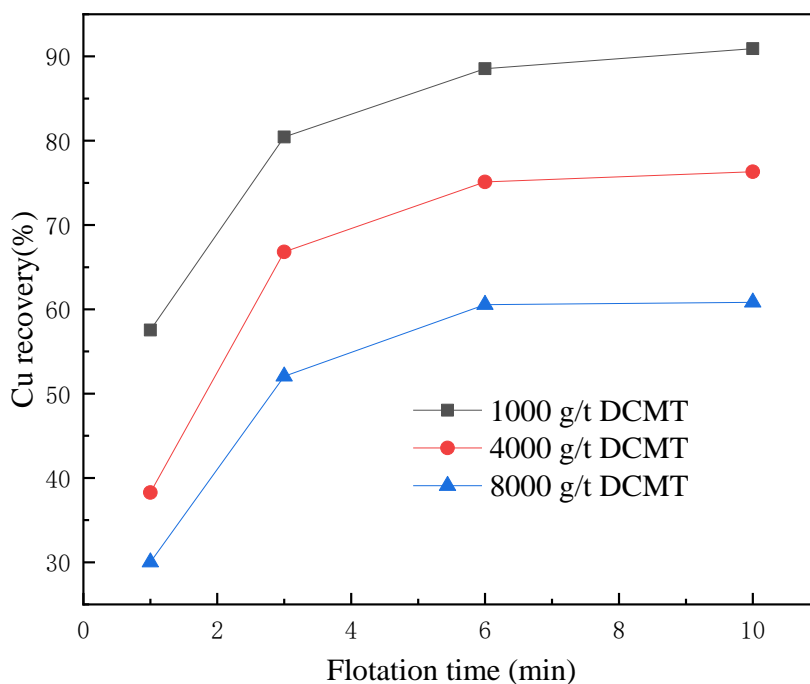


Figure 5. Chalcopyrite recovery as a function of flotation time at different DCMT dosages.

To verify the first conjecture, the changes in pH and Eh were monitored at different water hardness levels during the flotation period, as shown in Figure 6. Over time, the pH and Eh fluctuate in a soft water system. This is mainly related to the dissociation of carbonate in the solution. According to the relationship between the dissociation of the calcium carbonate solution and pH [32], carbonate ions generally begin to appear at a pH of approximately 8, and the solution has a buffering effect. Eh follows a similar trend to pH. Furthermore, when the dosage of calcium carbonate was equivalent to a hard water system, the pH/Eh difference was small, indicating that pH is not the main influencing factor.

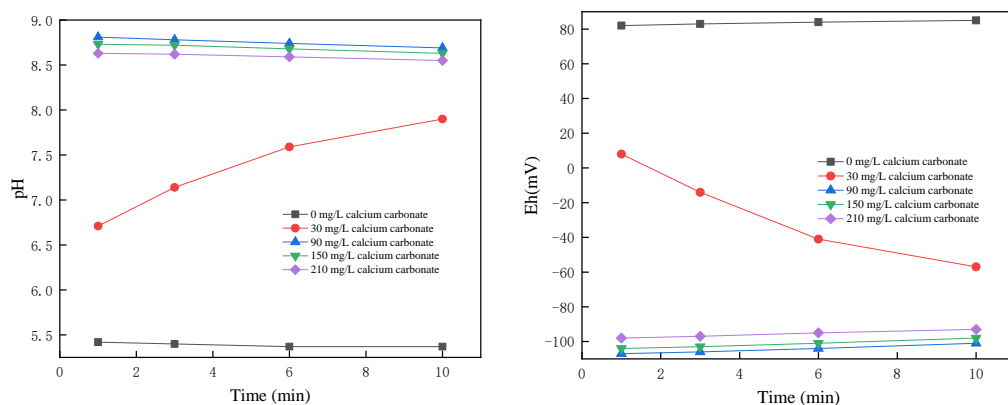


Figure 6. The pH and Eh as a function of flotation time in chalcopyrite flotation.

Spectroscopy and energy spectrum measurements were used for analysis and interpretation of the second conjecture.

3.2. Powder Contact Angle

Wettability is the most intuitive indication of mineral floatability [33]. To verify the flotation test results, contact angle testing was carried out. Because of the particularity of the ore sample, the powder contact angle test was considered the most appropriate. The test results shown in Figure 7 are consistent with the flotation results and confirm that an increase in the water hardness level improves the hydrophobicity of chalcopyrite. Notably, in the alcohol system, the rate at which the alcohol rose and wetted the chalcopyrite was fast, which differs from the previous results. This could indicate the presence of residual organic matter in the chalcopyrite because similar fast wetting speeds and miscibility are observed for organic compounds.

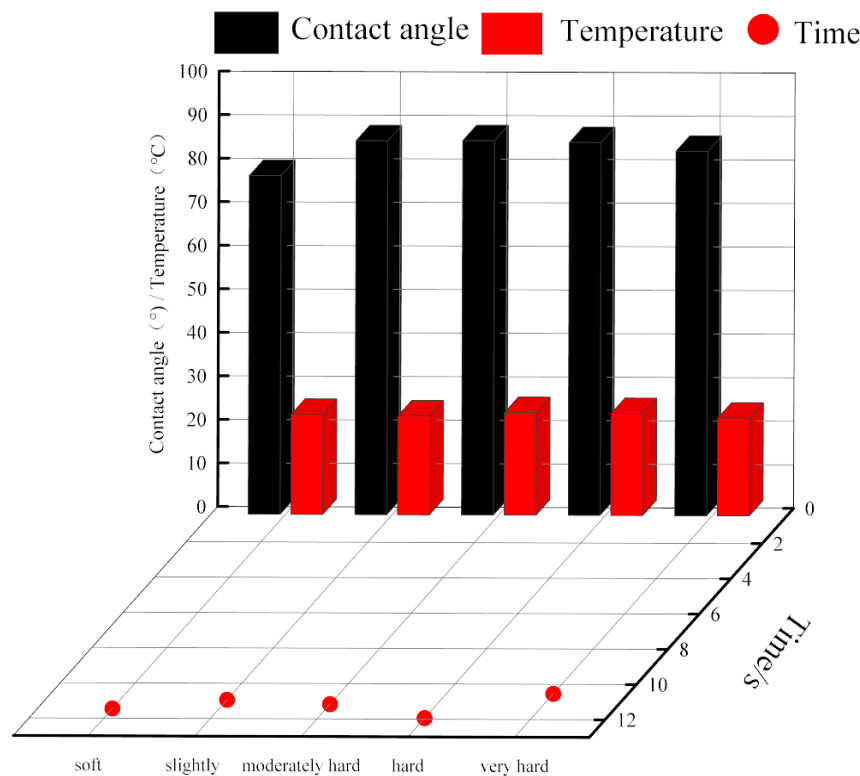


Figure 7. Powder contact angle.

3.3. FT-IR and Raman Spectra

A combination of infrared and Raman spectroscopy was used because the samples contain both inorganic (calcium carbonate) and organic compounds (starch and DCMT). The results are shown in Figures 8 and 9. The peaks at 1423 cm^{-1} , 875 cm^{-1} , and 714 cm^{-1} in the FT-IR spectrum of the sample after calcium carbonate was added are attributed to the ν_3 , ν_2 , and ν_4 vibration modes [34,35]. The peaks at 3000 cm^{-1} and 1799 cm^{-1} are attributed to a C-H stretching vibration [36,37], indicating that organic reagent (starch or xanthate) residue remains on the chalcopyrite. The Raman spectrum peaks at 500 cm^{-1} indicates that metals preferentially complex through M-O and M-C bonds [38,39]. Although there are no visible differences between the Raman spectra, parameters including the FWHM and integrated peak areas were different after fitting. The differences in the vibration intensities of calcium carbonate before and after the addition of DCMT indicate that the addition of DCMT led to a shedding of carbonate from the surface of the chalcopyrite. Therefore, it was inferred that the adsorption of calcium carbonate weakens the interaction between DCMT and chalcopyrite, thereby weakening the inhibition caused by DCMT. To explore the changes in metal elements, such as calcium ions, on the surface of chalcopyrite, an XPS analysis was conducted.

3.4. XPS

Figure 10 shows the scanning XPS for the binding energies of chalcopyrite before and after treatment. Figure 10b illustrates that the expected elements of Cu and S are present on the surface of chalcopyrite; however, due to oxidation, the O1s peak appears at approximately 531.93 eV in the spectrum [23,40]. After the chalcopyrite was treated with calcium carbonate, a new peak at approximately 346.43 eV was observed in the spectrum. This peak is assigned to Ca2p in calcium carbonate (Figure 10a). The spectrum of the sample after DCMT treatment contained a peak near 399.28 eV. This did not correspond to either calcium carbonate or DCMT, and was ascribed to N1s from a contaminant in the air. The surface atom concentration in the samples before and after treatment was different, as shown in Figure 10a,c, and Table 3. These results confirm that calcium carbonate is adsorbed on the surface of chalcopyrite.

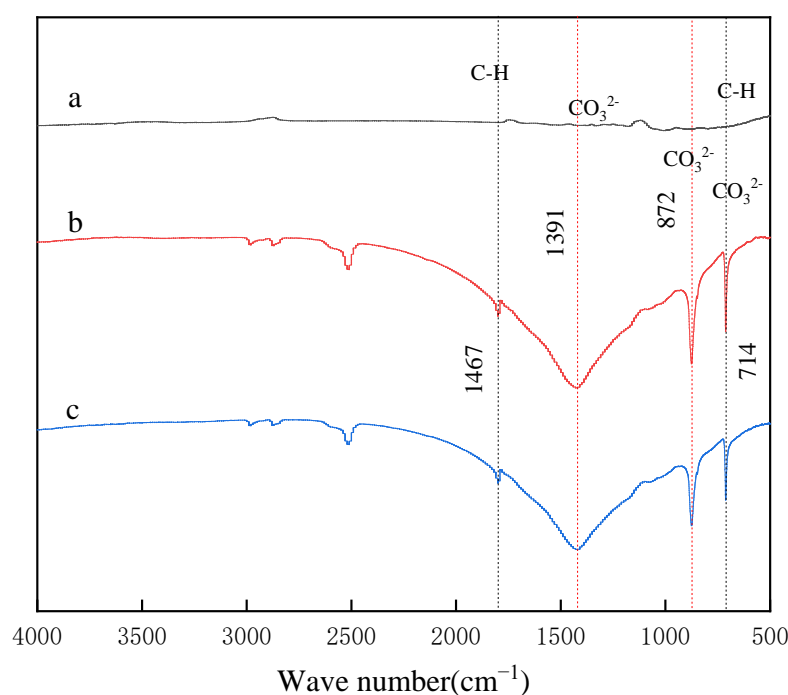


Figure 8. Fourier transform infrared spectroscopy in chalcopyrite (a) and chalcopyrite+calcium carbonate (b) and chalcopyrite+calcium carbonate+DCMT (c).

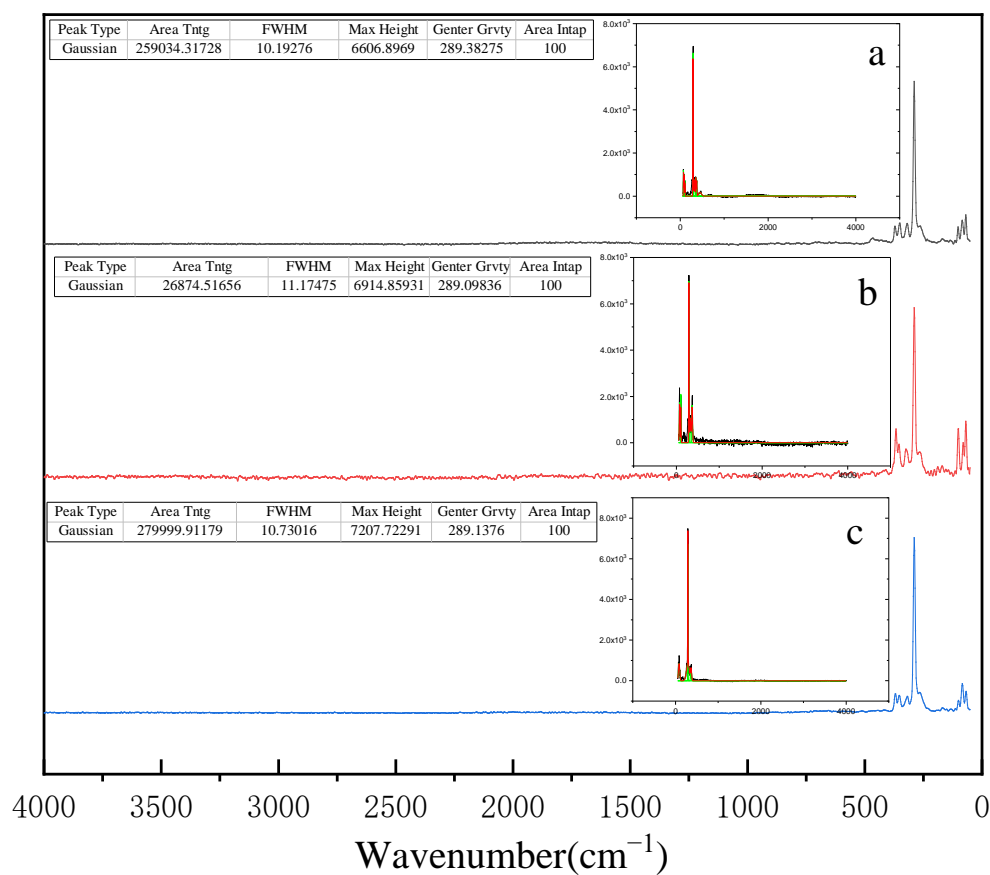


Figure 9. Raman spectra in chalcopyrite (a) and chalcopyrite+calcium carbonate (b) and chalcopyrite+calcium carbonate+DCMT (c).

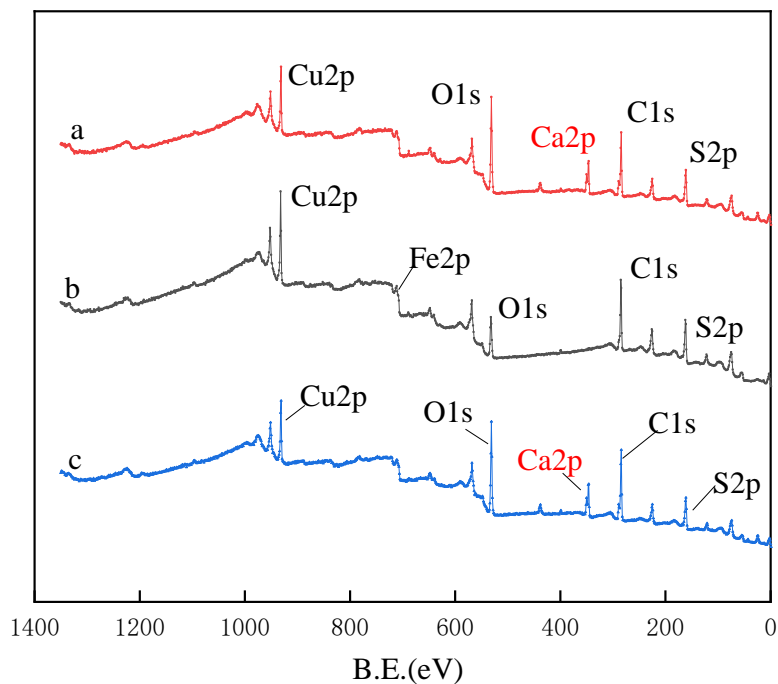


Figure 10. XPS in chalcopyrite (b) and chalcopyrite+calcium carbonate (a) and chalcopyrite+calcium carbonate+DCMT (c).

Table 3. Atomic concentration.

Chalcopyrite	Atomic Concentration/%				
	C1s	O1s	S2p	Cu2p	Ca2p
untreated	58.52	15.69	19.46	6.34	-
Treated by CaCO ₃	49.54	27.20	14.00	4.26	5.00
Treated by CaCO ₃ /DCMT	51.11	25.39	12.38	3.92	5.30

To further understand the valence states of the surface species, the fine XPS spectra of Cu2p and C1s were further analyzed, as shown in Figures 11 and 12.

Figure 11 shows the Cu2p spectra of chalcopyrite before and after treatment. The peak at 932.07 eV in the spectrum of the untreated chalcopyrite is assigned to Cu2p_{3/2}, which is consistent with previously reported results [23,41,42]. In the spectrum of the chalcopyrite treated with calcium carbonate, the Cu2p_{3/2} peak shifted toward a lower binding energy at 931.81 eV. The difference between the peak binding energies in the untreated and treated samples is 0.26 eV, indicating that the copper ion density in the treated chalcopyrite is higher. In the XPS spectra of calcium carbonate and DCMT, the Cu2p_{3/2} peak is located at 931.77 eV, which is 1.96 eV lower than that of previously reported DCMT peaks [18]. This indicates that the electron density of calcium carbonate and DCMT increased. These results indicate that the electronic contributions of calcium, carbon, and sulfur atoms in DCMT and calcium carbonate lead to an increase in the copper electron density, which confirms that calcium carbonate and DCMT are chemisorbed on the surface of chalcopyrite.

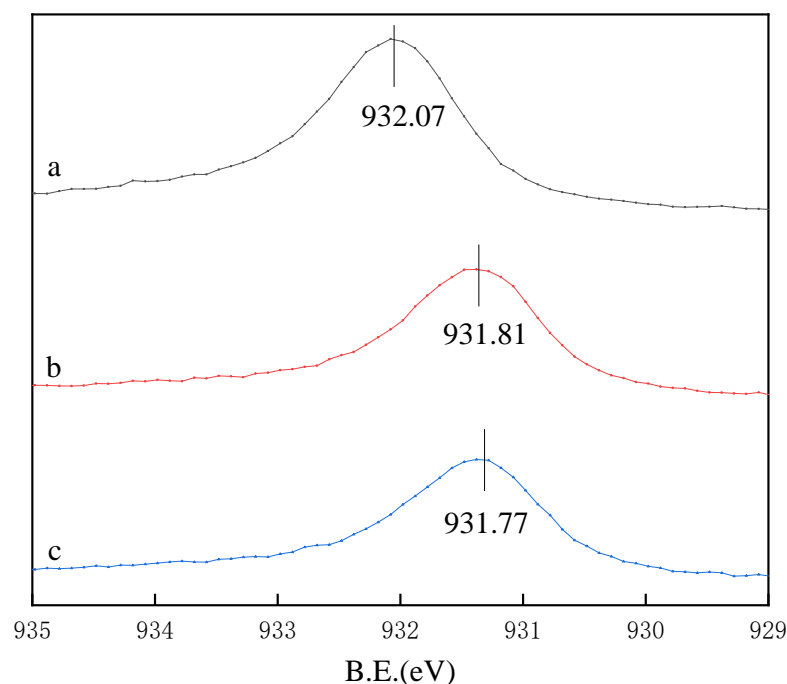


Figure 11. Cu2p XPS in chalcopyrite (a) and chalcopyrite+calcium carbonate (b) and chalcopyrite+calcium carbonate+DCMT (c).

The fine C1s spectra of chalcopyrite before and after treatment are shown in Figure 12. The peaks at 284.76 eV, 286.56 eV, and 288.51 eV in the C1s spectrum of the original chalcopyrite, which are assigned to C-C, C-O, and C=O, respectively, agree with previously reported XPS results [43]. The C1s spectrum of the treated chalcopyrite also includes C-C, C-O, and C=O peaks, but in different proportions to those seen on the untreated sample spectrum (Table 4). The higher proportions of carbon and oxygen indicate that carbonate is adsorbed on the surface of chalcopyrite. The addition of DCMT can reduce the proportion

of carbon and oxygen on the surface, indicating that there is a relationship between calcium carbonate and DCMT.

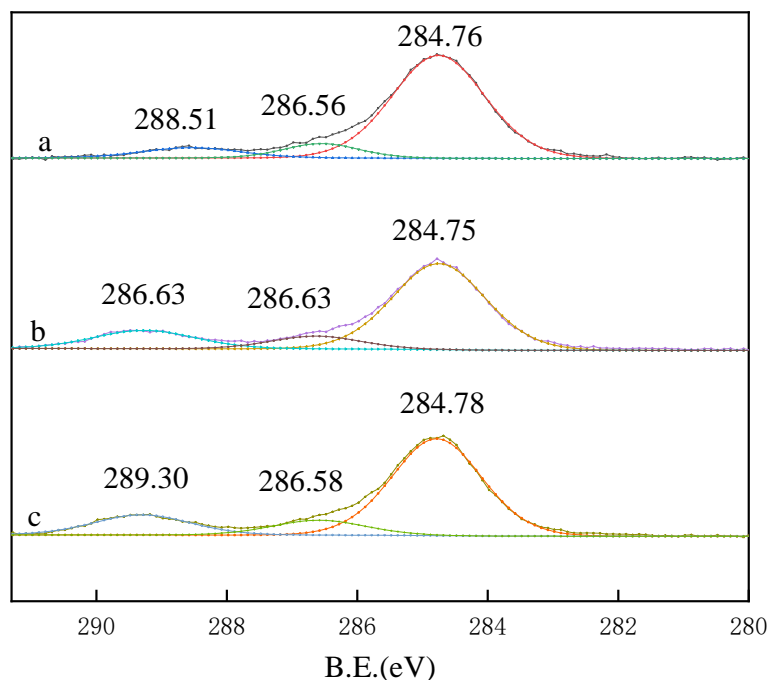


Figure 12. C1s XPS in chalcopyrite (a) and chalcopyrite+calcium carbonate (b) and chalcopyrite+calcium carbonate+DCMT (c).

Table 4. Percentage of binding energy.

Chalcopyrite	Concentration/%		
	C-C	C-O	C=O
untreated	81.78	8.27	9.96
Treated by CaCO ₃	72.64	10.41	16.95
Treated by CaCO ₃ /DCMT	72.41	11.46	16.12

4. Conclusions

Mixed copper concentrates obtained from the field can contain residual reagents on their surfaces; hence, the chalcopyrite was first pretreated in the laboratory. The influence of the water hardness level of the pulp on the inhibition of chalcopyrite by DCMT was studied using FT-IR, Raman spectroscopy, and XPS.

The flotation tests demonstrated that the inhibition effect of DCMT decreased as the water hardness level increased. In the DCMT system, the water hardness level increases from soft water to very hard water and the flotation recovery of chalcopyrite increases by about 10 percentage points. The results of the powder contact angle tests demonstrated that the water quality affected the inhibition ability of DCMT, which is consistent with the flotation results. The mechanism for the influence of water quality on DCMT was proposed and verified. An increase in the water hardness level caused an increase in the calcium ion concentration in the pulp, and through interactions with macromolecular agents such as starch, the calcium ions were adsorbed on the chalcopyrite, which weakened the inhibition effect of DCMT on chalcopyrite. However, the presence of DCMT reduced the concentration of calcium ions adsorbed on the chalcopyrite.

This study can serve as a guideline for the application of DCMT to industrial production. DCMT can be used to suppress the flotation of chalcopyrite and other sulfide ores and can be applied to copper–molybdenum separation. To achieve an optimal DCMT inhibition effect, the pulp water should contain negligible calcium carbonate, with the optimal level

being soft water. With increasing water hardness levels, the higher levels of calcium ions will weaken the inhibition effect of DCMT on chalcopyrite and reduce the floatability of molybdenite, which is not conducive to the separation of these minerals.

Flotation agents can also reduce the water hardness level by adsorbing ions in the water, which reduces the water hardness level and regulates the flotation via the ions in the water to achieve multiple benefits from a single reagent. The effect of ions from the dissolution of vein minerals on flotation chemicals should also be noted.

Author Contributions: Conceptualization, Y.S., W.Q. and L.C.; Data curation, Y.W. and W.W.; Formal analysis, W.W.; Funding acquisition, L.C.; Investigation, W.W. and Y.S.; Methodology, Y.W., Y.S., W.Q. and L.C.; Resources, Y.S.; Software, Y.W.; Supervision, W.Q.; Validation, Y.W. and W.W.; Writing—original draft, Y.W.; Writing—review and editing, Y.S. and L.C. All authors have read and agreed to the published version of the manuscript.

Funding: This work was supported by High-Level Talent Recruitment Program of Yunnan Province (No. CCC21321005A).

Data Availability Statement: No new data were created or analyzed in this study.

Conflicts of Interest: The authors declare that they have no known competing financial interests or personal relationships that could have appeared to influence the work reported in this paper.

References

- Ozkan, S.G.; Acar, A. Investigation of impact of water type on borate ore flotation. *Water Res.* **2004**, *38*, 1773–1778. [[CrossRef](#)]
- Aliaskari, M.; Schaefer, A.I. Nitrate, arsenic and fluoride removal by electro dialysis from brackish groundwater. *Water Res.* **2022**, *190*, 116683. [[CrossRef](#)]
- Zhiyao, Z.; Yuqin, Z.; Xiaoyi, W.; Zhaoyang, W.; Yuting, B. Water quality evolution mechanism modeling and health risk assessment based on stochastic hybrid dynamic systems. *Expert Syst. Appl.* **2022**, *193*, 116406. [[CrossRef](#)]
- Nong, X.; Shao, D.; Zhong, H.; Liang, J. Evaluation of water quality in the South-to-North Water Diversion Project of China using the water quality index (WQI) method. *Water Res.* **2020**, *178*, 115781. [[CrossRef](#)]
- Wang, J.; Liao, R.; Tao, L.; Zhao, H.; Zhai, R.; Qin, W.; Qiu, G. A comprehensive utilization of silver-bearing solid wastes in chalcopyrite bioleaching. *Hydrometallurgy* **2017**, *169*, 152–157. [[CrossRef](#)]
- Ukubuiwe, A.C.; Olayemi, I.K.; Arimoro, F.O.; Omalu IC, J.; Ukubuiwe, C.C.; Baba, B.M.; Sule, B.U. Effects of water hardness level on metabolic reserves of post-embryonic life stages of *Culex quinquefasciatus* Say 1826 (Diptera: Culicidae). *Int. J. Trop. Insect Sci.* **2021**, *42*, 1297–1306. [[CrossRef](#)]
- Wonder, C.; Yongjun, P. Selective inhibition of kaolinite entrainment during chalcopyrite flotation in saline water. *Miner. Eng.* **2022**, *184*, 107637.
- Chen, Y.; Chen, X.; Peng, Y. The effect of sodium hydrosulfide on molybdenite flotation in seawater and diluted seawater. *Miner. Eng.* **2020**, *158*, 106589. [[CrossRef](#)]
- Hamilton, T.; Huai, Y.; Peng, Y. Lead adsorption on copper sulphides and the relevance to its contamination in copper concentrates. *Miner. Eng.* **2020**, *154*, 106381. [[CrossRef](#)]
- Weiming, W.; Tao, C.; Yanhai, S.; Guohua, Y.; Xiong, T. The flotation separation of molybdenite from talc using zinc sulfate in sodium silicate system and related mechanism. *Colloids Surf. A Physicochem. Eng. Asp.* **2022**, *641*, 128451.
- Changtao, W.; Runqing, L.; Meirong, W.; Zhijie, X.; Mengjie, T.; Zhigang, Y.; Wei, S.; Chenyang, Z. Flotation separation of molybdenite from chalcopyrite using rhodanine-3-acetic acid as a novel and effective depressant. *Miner. Eng.* **2021**, *162*, 106747.
- Ikumapayi, F.; Rao, K.H. Recycling Process Water in Complex Sulfide Ore Flotation: Effect of Calcium and Sulfate on Sulfide Minerals Recovery. *Miner. Process. Extr. Metall. Rev.* **2015**, *36*, 45–64. [[CrossRef](#)]
- Chen, J.-H.; Lan, L.-H.; Liao, X.-J. Depression effect of pseudo glycolthiourea acid in flotation separation of copper–molybdenum. *Trans. Nonferrous Met. Soc. China* **2013**, *23*, 824–831. [[CrossRef](#)]
- Zhigang, Y.; Yuehua, H.; Wei, S.; Chenyang, Z.; Jianyong, H.; Zhijie, X.; Jingxiang, Z.; Changping, G.; Chenhu, Z.; Qingjun, G.; et al. Adsorption Mechanism of 4-Amino-5-mercaptop-1,2,4-triazole as Flotation Reagent on Chalcopyrite. *Langmuir ACS J. Surf. Colloids* **2018**, *34*, 4071–4083.
- Yin, Z.-G.; Sun, W.; Hu, Y.-H.; Guan, Q.-J.; Zhang, C.-H.; Gao, Y.-S.; Zhai, J.-H. Depressing behaviors and mechanism of disodium bis (carboxymethyl) trithiocarbonate on separation of chalcopyrite and molybdenite. *Trans. Nonferrous Met. Soc. China* **2017**, *27*, 883–890. [[CrossRef](#)]
- Roman, O.; Lesyk, R. Synthesis and anticancer activity in vitro of some 2-thioxo-4-thiazolidone derivatives. *Farmacia* **2007**, *55*, 640–648.
- Bresson, C.R.; Parlman, R.M.; Kimble, J.B. Trithiocarbonate Flotation Reagents. U.S. Patent No 4,561,984, 31 December 1985.
- Timbillah, S. Mechanism for Disodium Carboxymethyl Trithiocarbonate (Orfom[®] D8) Depression in Chalcopyrite-Molybdenite Flotation Systems. Ph.D. Thesis, Montana Technological University, Butte, MT, USA, 2019.

19. Timbillah, S.; Fosu, B.; Lan, P.L.; Sosa-Blanco, C.; Hill, L. Towards an Understanding of the Use of Disodium Carboxymethyl Trithiocarbonate (DCMT) as an Alternative Depressant in Cu/Mo Sulfide Flotation. *Min. Metall. Explor.* **2021**, *38*, 1–14. [[CrossRef](#)]
20. Yin, Z.; Sun, W.; Hu, Y.; Zhai, J.; Qingjun, G. Evaluation of the replacement of NaCN with depressant mixtures in the separation of copper–molybdenum sulphide ore by flotation. *Sep. Purif. Technol.* **2017**, *173*, 9–16. [[CrossRef](#)]
21. Timbillah, S.; Young, C.; Das, A. Understanding the Electrochemical Behavior of Di-Sodium Carboxymethyl Trithiocarbonate (Orfom[®] D8) Depressant on Copper Metal and Chalcopyrite Surfaces. *Meet. Abstr.* **2018**, *MA2018–01*, 2153. [[CrossRef](#)]
22. Christian, U.A.; Kayode, O.I.; James, O.I.C.; Ofurum, A.F.; Catherine, U.C. Morphometric diagnosis of the effects of water hardness on development of immature life stages and adult vectorial fitness of *Culex quinquefasciatus* (Diptera: *Culicidae*) mosquito. *Zoomorphology* **2018**, *137*, 511–518.
23. Zhang, X.; Lu, L.; Cao, Y.; Yang, J.; Che, W.; Jiongtian, L. The flotation separation of molybdenite from chalcopyrite using a polymer depressant and insights to its adsorption mechanism. *Chem. Eng. J.* **2020**, *395*, 125137. [[CrossRef](#)]
24. Liao, R.; Feng, Q.; Wen, S.; Liu, J. Flotation separation of molybdenite from chalcopyrite using ferrate(VI) as selective depressant in the absence of a collector. *Miner. Eng.* **2020**, *152*, 106369. [[CrossRef](#)]
25. Guangsheng, Z.; Leming, O.; Wencai, Z.; Yuteng, Z. Effects of Sodium Alginate on the Flotation Separation of Molybdenite From Chalcopyrite Using Kerosene as Collector. *Front. Chem.* **2020**, *8*, 242.
26. Fu, Y.; Zhu, Z.; Yao, J.; Han, H.; Yin, W.; Yang, B. Improved depression of talc in chalcopyrite flotation using a novel depressant combination of calcium ions and sodium lignosulfonate. *Colloids Surf. A Physicochem. Eng. Asp.* **2018**, *558*, 88–94. [[CrossRef](#)]
27. Binbin, L.; Dezhi, L.; Saizhen, J.; Qingyun, L.; Zejun, W. The effect of nascent calcium carbonate inhibiting the flotation behavior of calcite. *Miner. Eng.* **2022**, *180*, 107478.
28. Changbin, L.; Qing, S.; Guofan, Z.; Hongjiang, L.; Haigang, F. Effect of aluminum ions on the adsorption of carboxymethyl cellulose onto talc. *Miner. Eng.* **2021**, *170*, 107018.
29. Yann, F.; Lev, F.; Inna, F.; Michael, B. The Challenge of Tungsten Skarn Processing by Froth Flotation: A Review. *Front. Chem.* **2020**, *8*, 230.
30. Chimonyo, W.; Fletcher, B.; Peng, Y. The differential depression of an oxidized starch on the flotation of chalcopyrite and graphite. *Miner. Eng.* **2020**, *146*, 106114. [[CrossRef](#)]
31. Rath, R.K.; Subramanian, S.; Pradeep, T. Surface Chemical Studies on Pyrite in the Presence of Polysaccharide-Based Flotation Depressants. *J. Colloid Interface Sci.* **2000**, *229*, 82–91. [[CrossRef](#)]
32. Feng, B.; Luo, X.-P. The solution chemistry of carbonate and implications for pyrite flotation. *Miner. Eng.* **2013**, *53*, 181–183. [[CrossRef](#)]
33. Wang, X.; Zhang, Q. Role of surface roughness in the wettability, surface energy and flotation kinetics of calcite. *Powder Technol.* **2020**, *371*, 55–63. [[CrossRef](#)]
34. Taylor, E.A.; Mileti, C.J.; Ganesan, S.; Kim, J.H.; Donnelly, E. Measures of Bone Mineral Carbonate Content and Mineral Maturity/Crystallinity for FT-IR and Raman Spectroscopic Imaging Differentially Relate to Physical–Chemical Properties of Carbonate-Substituted Hydroxyapatite. *Calcif. Tissue Int.* **2021**, *109*, 77–91. [[CrossRef](#)]
35. Serna, C.J.; White, J.L.; Hem, S.L. Structural Survey of Carbonate-Containing Antacids. *J. Pharm. Sci.* **1978**, *67*, 324–327. [[CrossRef](#)] [[PubMed](#)]
36. Young, R.D.; Hill, A.F.; Hillier, W.; Ball, G.E. Transition metal-alkane θ -complexes with oxygen donor Co-ligands. *J. Am. Chem. Soc.* **2011**, *133*, 13806–13809. [[CrossRef](#)]
37. Williams, S.D.; Johnson, T.J.; Sharpe, S.W.; Oates, R.P.; Brauer, C.S. Quantitative vapor-phase IR intensities and DFT computations to predict absolute IR spectra based on molecular structure: I. Alkanes. *J. Quant. Spectrosc. Radiat. Transf.* **2013**, *129*, 298–307. [[CrossRef](#)]
38. Hanna, S.; Wojciech, C.; Piotr, T. Starch-metal complexes and metal compounds. *J. Sci. Food Agric.* **2018**, *98*, 2845–2856.
39. Kazuo, N. *Infrared and Raman Spectra of Inorganic and Coordination Compounds*, 4th ed.; John Wiley & Sons: Hoboken, NJ, USA, 1986.
40. Mielczarski, J.A.; Cases, J.M.; Alnot, M.; Ehrhardt, J.J. XPS Characterization of Chalcopyrite, Tetrahedrite, and Tennantite Surface Products after Different Conditioning. 1. Aqueous Solution at pH 10. *Langmuir* **1996**, *12*, 2519–2530. [[CrossRef](#)]
41. Liu, G.; Qiu, Z.; Wang, J.; Liu, Q.; Xiao, J.; Zeng, H.; Zhong, H.; Xu, Z. Study of N-isopropoxypropyl-N'-ethoxycarbonyl thiourea adsorption on chalcopyrite using in situ SECM, ToF-SIMS and XPS. *J. Colloid Interface Sci.* **2015**, *437*, 42–49. [[CrossRef](#)]
42. Zuyuan, T.; Haodong, L.; Qian, W.; Wenqing, Q.; Congren, Y. Effects of redox potential on chalcopyrite leaching: An overview. *Miner. Eng.* **2021**, *172*, 107135.
43. Chastain, J.; King, R.C. (Eds.) *Handbook of X-Ray Photoelectron Spectroscopy: A Reference Book of Standard Spectra for Identification and Interpretation of XPS Data*; Physical Electronics: Eden Prairie, MN, USA, 1995.

Disclaimer/Publisher's Note: The statements, opinions and data contained in all publications are solely those of the individual author(s) and contributor(s) and not of MDPI and/or the editor(s). MDPI and/or the editor(s) disclaim responsibility for any injury to people or property resulting from any ideas, methods, instructions or products referred to in the content.